

Design of a Beam Phase Measurement and Selection System for the M.S.U. K500 Cyclotron,\*

B. Milton, M. Fowler, J. Kuchar, and R.M. Ronningen  
National Superconducting Cyclotron Laboratory Michigan State University, East Lansing, Michigan, 48824

Abstract

We are currently constructing equipment to measure the phase of the internal beam. One device is a plastic scintillator in the magnet which will detect gamma rays emitted when the beam hits the main probe. By measuring the time of the Y's relative to the rf time the phase of the beam at the probe radius is determined. We are also designing an internal phase selection system which will work on principals similar to those of the K50 system. Both new systems are constrained by the compact geometry of the K500. In this paper, we will discuss the resolution of these difficulties and present preliminary results of the phase measurements.

Phase Measurement

The K500 cyclotron currently in operation at Michigan State University is constructed with a yoke which has cylindrical symmetry in the median plane<sup>1</sup>, except for a few small penetrations for diagnostic equipment. These access holes are limited by the space between the main coils. Our goal is to measure the beam phase and phase width as a function of radius. One way to do this is to measure the time of arrival of gamma rays versus the rf time. Since these gammas are being produced by the beam hitting the main probe their time structure should accurately reflect the time structure of the beam. Unfortunately the small median plane penetration acts as an extremely good collimator and in our first prototype the main probe was only visible for a few inches of travel. A solution to this problem was to get the detector closer to the beam chamber. This layout is shown in figure 3. The high field (50 kg) in this region precluded the use of semi-conductors or other electronics, so we placed a plastic scintillator in the viewport hole at the liner, i.e., as close to the beam as possible. A glass rod transmits the light pulses to a photomultiplier located at the edge of the yoke where it could be adequately shielded from the the field. The anode signal is then passed through a constant fraction timing discriminator (CFD). Low energy events, randoms, and the detector noise are minimized by the threshold adjustment. This signal is then used as a start signal for a time to pulse height converter (TAC). The stop signal is a pulse every second (positive slope) zero crossing of the rf signal. The output of the TAC is fed into a pulse height analyzer. A typical spectrum (collected for 200 seconds) is shown in figure 1. In this case the primary peak appears twice, a consequence of the divide-by-two on the stop signal from the rf, and it allows easy calibration since the two peaks are separated by exactly 360 rf degrees. This figure also shows several smaller peaks at very different parts of the rf cycle. These peaks are due to various beam losses at angles other than that of the probe. In figure 2 a spectrum from a different beam is shown for the same beam energy. In this case the beam loss mechanisms clearly dominate the spectrum, suggesting charge stripping. These loss peaks occur at distinct

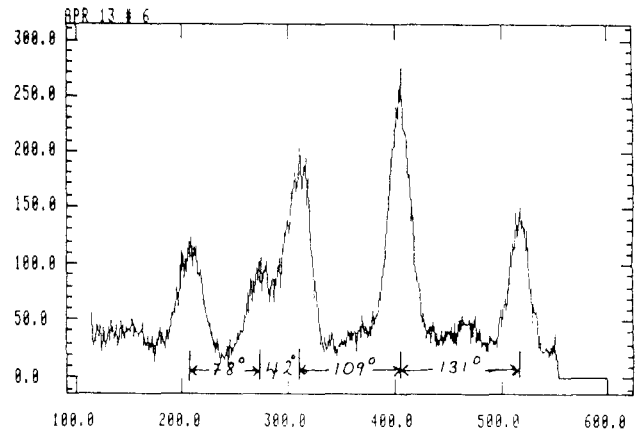


Fig. 1 Time spectrum collected when 20 MeV/A <sup>4</sup>He<sup>1+</sup> was hitting a probe at 25 inches. The two primary peaks are 360° in rf time apart allowing easy calibration. The phase width (FWHM) of the beam is 30°. The smaller peaks are due to unknown beam loss mechanisms.

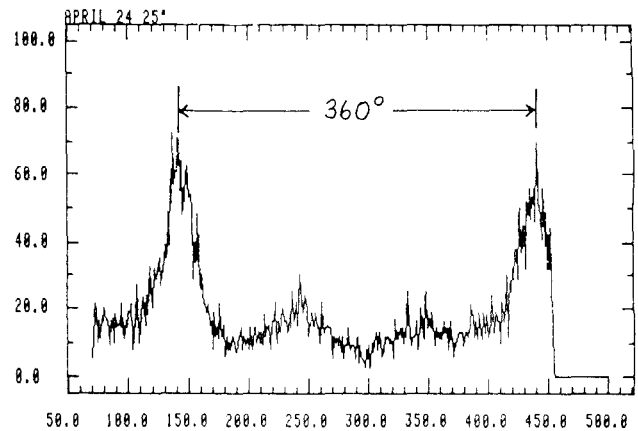


Fig. 2 Time spectrum collected when <sup>14</sup>N<sup>4+</sup> was hitting the main probe at 26 inches. The peak due to the main probe appears to be buried under peaks caused by an as yet unexplained loss mechanism. The loss peaks each appear when the probe is at different radii.

radii and are tunable with machine parameters such as the first harmonic bump.

We are currently investigating these and other sources of correlated time structures in order to understand their origin and behavior. It should be

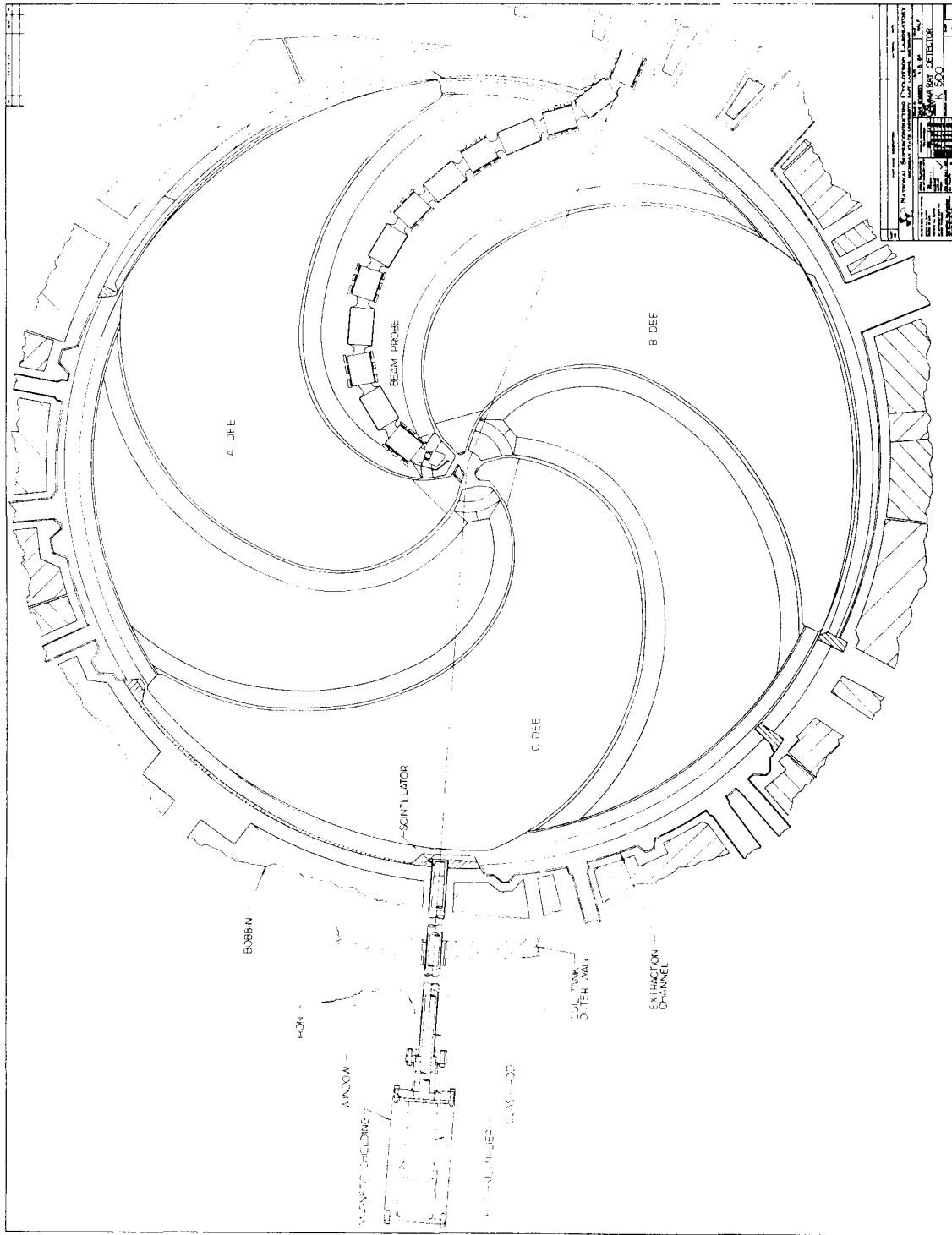


Fig. 3 Median plane layout geometry showing arrangement of the gamma-ray detector components, and the location of the main probe at it's inner most position. Gamma rays are produced when the beam hits the main probe. These are then detected by the plastic scintillator, and the light pulses are transmitted by a one meter long glass light pipe to a photo-multiplier tube. Their time of arrival is measured relative to the rf time giving a measurement of the time of arrival of the beam at the probe. This in turn is a measure of the phase and phase width of the beam at the probe angle and radius.

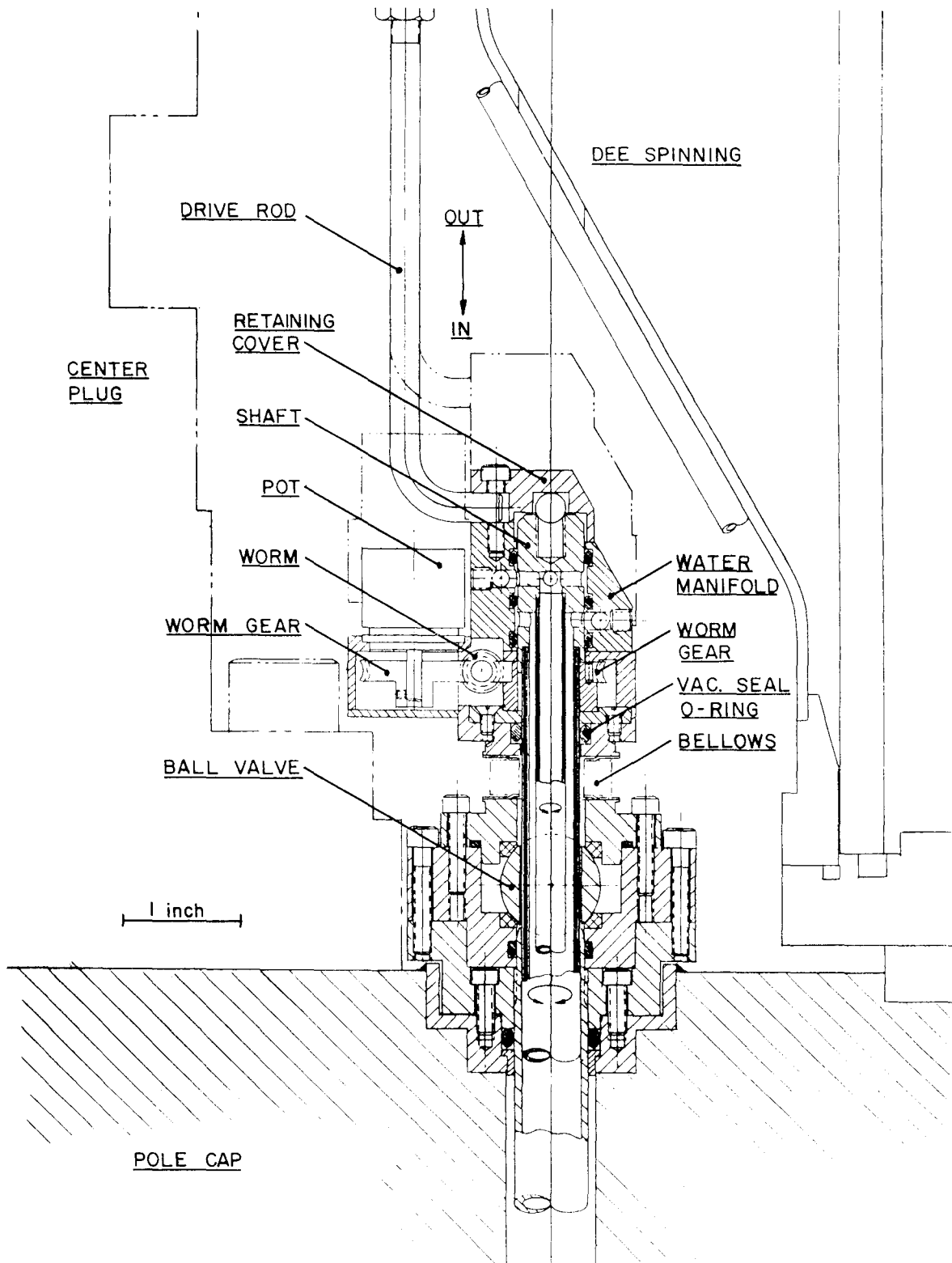


Fig. 4 Mechanical design of the drive mechanism for the K500 phase slits, showing spatial constraints on the vacuum lock, water manifold, and rotational drive. The worm is driven by a stepping motor mounted several feet away, the two being connected by a flexible drive cable. The vacuum lock is provided by the small manually operated ball valve. Removal of the blade requires the insertion of a rod through the dee stem which to be attached to the top of the shaft. This rod is then used to pull the shaft out through the spinning, while the water manifold and rotational drive remain in place.

noted that beam losses, and the necessity of the beam being at sufficient energy to penetrate the Coulomb barrier, limit the utility of this technique, but the relative ease of setup and low cost make it an attractive first step in gaining information about the beam phase history.

#### Phase Selection

As demonstrated in K50 cyclotron operation<sup>2</sup> a phase selection system is a highly effective method of producing beams with high energy resolution. It also reduces the activation of the internal components such as the deflector. The principle of operation of such a system<sup>2</sup> is to use the phase-dependent centering error to spatially separate different phases and then remove the unwanted beam with a physical obstruction. If this is done before the particles reach the Coulomb barrier then the activation which would have occurred from the 'phase selection' at the deflector septum, is avoided. Conceptually two movable blades located at 7.038 inches in radius and at the center of two successive hills provide the obstructions. This radius corresponds to turn number 32 in first harmonic (fixed turn number) geometry, where the turn separation is of the order of 10 mils. This small turn separation removes the possibility of using a slit as was done in the K50. One blade will be placed between turn 31 and turn 32. Another will be located on the next hill between turns 32 and 33. Given proper selection of the phase curve and beam centering using the harmonic bump coil, this method should allow the selection of a beam with a much smaller phase spread than the 30 degrees we have currently. Our access to the median plane for such a device is restricted to two vertical, one-half inch diameter holes. One is in the upper, and the other in the lower, pole cap. In order to provide sufficient mobility each blade will be mounted off-center at the end of a forty inch water-cooled copper rod. By rotating the rod the position of the blade can be varied by  $\pm 1/4$  inches in radius.

In figure 4 the mechanical design for the drive mechanism, located under the dee stem spinning at the top end of the shaft, is shown. This mechanism must provide the airlock to allow removal under vacuum, the rotational drive, and provide the in-out motion necessary to insert and remove the blade from the

beam. Pulling the rod up one inch will remove the blade from the beam chamber. The blades will thus be mounted on a removable cap fitted on the end of the copper shaft, held in place with a set screw. Once the shaft has been pulled completely out of the magnet the blades can be easily changed. To vary the radius of the blade the shaft is rotated by a worm gear mounted concentrically on the shaft and a worm mounted in the body of the mechanism. A similar gear driven off the same worm connects to an encoder potentiometer. Since the pot has no end stops, and the water manifold has rotating seals, the shaft can be rotated any number of full turns in either direction. The worm will be driven by a stepping motor located several feet off the pole cap on the rf support structure, to keep the motor away from fringe fields and to minimize space utilization. The worm and motor will be connected by a flexible drive cable, but since the encoder reads directly off the worm, cable backlash should not influence the positioning accuracy of the blade. The in-out motion uses a small air cylinder mounted on the top of the dee spinning, and connects to the top of the water manifold by a hooked drive rod. During in-out travel the bellows provides the vacuum seal. The manifold section above the bellows travels on two guide rods to maintain the alignment to the hole.

The airlock is achieved with the ball valve located at the top of the hole, and the bellows above it. When the bellows are stretched (blade in an out position) the space between the ball and the sliding O-ring, above the bellows, is large enough to accommodate the blade portion of the shaft. Removal will consist of inserting a rod through the dee stem spinning and attaching it to the top of the shaft, which is exposed when the retaining cover is removed. The shaft will then be pulled up through the spinning while the water manifold and drive mechanism remain in place. The vacuum is maintained by the sliding O-ring. When the blade has cleared the ball valve can be closed and the shaft can be withdrawn the rest of the way.

#### References

- \* Work supported by NSF under Grant No. PHY-83-12245.
- 1. MSUCP-30, 1980.
- 2. H.G. Blosser, 1969 cyclotron conference, page 257.